Band Gaps in a Multiresonator Acoustic Metamaterial

G. L. Huang[1]
Department of Systems Engineering,
University of Arkansas at Little Rock,
Little Rock, AR 72204
e-mail: glhuang@ualr.edu

C. T. Sun
School of Aeronautics and Astronautics,
Purdue University,
W. Lafayette, IN 47907

In this study, we investigated dispersion curves and the band gap structure of a multiresonator mass-in-mass lattice system. The unit cell of the lattice system consists of three separate masses connected by linear springs. It was demonstrated that the band gaps can be shifted by varying the spring constant and the magnitude of the internal masses. By using the conventional monatomic (single mass) lattice model as an equivalent system, the effective mass was found to become negative for frequencies in the band gaps. An attempt was made to represent the two-resonator mass-in-mass lattice with a microstructure continuum model. It was found that the microstructure continuum model can capture the dispersive behavior and band gap structure of the original two-resonator mass-in-mass system. [DOI: 10.1115/1.4000784]

Keywords: acoustic metamaterials, band gap, dispersion curves, negative effective mass, microstructure continuum theory

1 Introduction

Recently, many researchers were engaged in exploring electromagnetic metamaterials [1–3] with unusual properties such as a negative refractive index for various novel applications [4–6]. The photonic band gap, a range of frequency in which electromagnetic waves cannot propagate, is of interest to engineers in designing photonic devices [7]. Because of the similarity between stress wave propagation in phononic crystals and electromagnetic waves in photonic crystals [8–10], acoustic metamaterials that contain manmade periodic microstructures also attracted much attention recently. Practical applications of these systems include mechanical filters, sound and vibration isolators, and acoustic waveguides [11,12]. One of the most attractive features in acoustic metamaterials is the possibility to tailor the desired band gap for stopping propagation of waves of certain frequencies, especially for the construction of the low frequency band gap.

Many researches about band gaps of acoustic and elastic wave propagation in phononic crystals have been conducted, both theoretically and experimentally. One of the first calculations of acoustic band gaps in a simple periodic composite was performed by Kushwaha et al. [13]. However, the calculation in Ref. [13] was carried out only for the case of antiplane shear. By using mechanical lattice structures, complete acoustic band gaps were demonstrated by Martinsson and Movchan [14], who provided a method that can quickly determine band gaps. Using the plane-wave expansion method, the propagation of elastic waves through two-dimensional (2D) periodic composites, which exhibit full band gaps, was investigated [15]. However, it should be mentioned that the above studies about the acoustic band gaps are of the Bragg type, which appears at about an angular frequency ω of the order of v/a (v is the wave velocity and a is the periodic constant). Recently, studies of the acoustic metamaterials showed that the resonance phononic crystals can be designed to display some novel sonic properties such as refractionlike beam bending or refocusing [16–18]. Different from the Bragg type, the resonance phononic crystals (acoustic metamaterials) show that the size of the periodic constant could be much smaller than the wavelength of the wave at the low frequency band gap [19,20]. The negative refractive behavior for the acoustic wave in metamaterials can be described by introducing a negative effective mass density and/or modulus [21,22]. The negative effective mass density arises from the negative momentum of the unit cell with positive velocity fields due to local resonance, which was confirmed both experimentally [23]. It was demonstrated that the effective mass density becomes negative, owing to the local resonance of the internal masses.

The physical mechanism of the negative effect mass density can be also well understood with the help of a simple mass-spring structure. Recently, a one-resonator mass-in-mass lattice model was studied by Huang et al. [24] to understand the physical meaning of negative effective mass density and the corresponding stopping bands. The model is similar to the one originally introduced by Vincent [25] and more recently by Lazarov and Janson [26], to be used as a possible mechanical filter. However, the aforementioned systems, in general, have only two complete band gaps and may not be suitable for some device applications, which need multiple band gaps. In order to design multiple band gaps at the desired frequency range, a multiresonator mass-in-mass system is needed.

In this study, we demonstrated that, with multiresonator mass-in-mass lattice systems, there are several band gaps. Furthermore, these band gaps may be varied by changing the resonance frequencies of the resonators. It was also found that if the multiresonator system is represented by a monatomic (single mass) lattice system, then the effective lattice mass has to be frequency-dependent and, in the band gap, it becomes negative. The relationship between the negative effective mass and wave propagation in the lattice system was discussed. Finally, we employed a microstructure continuum model [27,28] to represent the multiresonator lattice system, and found that the microstructure continuum model is suitable for describing the wave motion and band structure of multiresonator lattice systems without the need of using negative masses.

2 Band Gaps in Multiresonator Acoustic Metamaterials

2.1 Two-Resonator Mass-in-Mass System. Consider an infinitely long one-dimensional lattice consisting of mass-in-mass units, as shown in Fig. 1. The unit-cells are placed periodically at a spacing of L. The three rigid masses are denoted as m_1, m_2, and m_3, from outside to inside of the unit cell, respectively. The three spring constants k_1, k_2, and k_3 are assumed to represent the respective interactions among the three masses. Note that, in each unit

[1]Corresponding author.

Contributed by the Technical Committee on Vibration and Sound of ASME for publication in the JOURNAL OF VIBRATION AND ACOUSTICS. Manuscript received March 11, 2009; final manuscript received October 8, 2009; published online April 14, 2010. Assoc. Editor: Stephen A. Hambric.

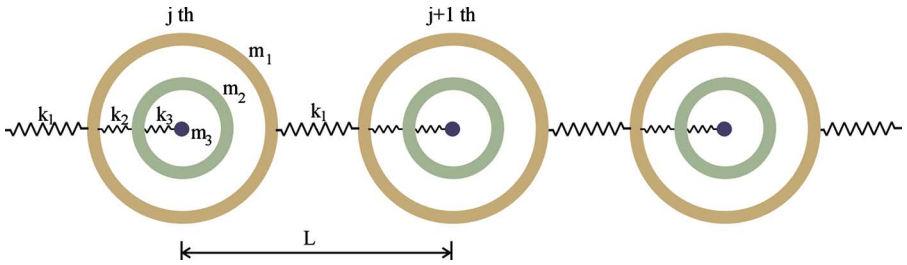

Fig. 1 The two-resonator mass-in-mass lattice structure

cell, there are two local resonators. This model is the extension of the one-resonator mass-in-mass model recently proposed by Huang et al. [24]

For the harmonic wave propagation in the two-resonator mass-in-mass lattice system, the equations of motion for the j-th unit cell can be expressed as

$$m_1\frac{d^2u_1^{(j)}}{dt^2} + k_1(2u_1^{(j)} - u_1^{(j-1)} - u_1^{(j+1)}) + k_2(u_1^{(j)} - u_2^{(j)}) = 0 \quad (1)$$

$$m_2\frac{d^2u_2^{(j)}}{dt^2} + k_2(u_2^{(j)} - u_1^{(j)}) + k_3(u_2^{(j)} - u_3^{(j)}) = 0 \quad (2)$$

$$m_3\frac{d^2u_3^{(j)}}{dt^2} + k_3(u_3^{(j)} - u_2^{(j)}) = 0 \quad (3)$$

where $u_\alpha^{(j)}$ represents the displacement of mass "α" in the j-th cell. The harmonic waveform of the displacement at the j-th cell for stationary response is

$$u_\alpha^{(j)} = B_\alpha e^{i(qx-\omega t)} \quad (4)$$

where B_α is the complex wave amplitude, q is the wave number, ω is the angular frequency, and $\alpha=1$, 2, and 3, denoting the three masses. Based on Eq. (4), the harmonic wave solution for the $(j+n)$-th cell for stationary response can then be expressed as

$$u_\alpha^{(j+n)} = B_\alpha e^{i(qx+nqL-\omega t)} \quad (5)$$

Substitution of Eqs. (4) and (5) with $n=1$ or -1 into Eqs. (1)–(3) yields three homogeneous equations for B_1, B_2, and B_3 as

$$\begin{bmatrix} 2k_1(1-\cos qL) + k_2 - m_1\omega^2 & -k_2 & 0 \\ -k_2 & k_2 + k_3 - m_2\omega^2 & -k_3 \\ 0 & -k_3 & k_3 - m_3\omega^2 \end{bmatrix}\begin{Bmatrix} B_1 \\ B_2 \\ B_3 \end{Bmatrix} = \begin{Bmatrix} 0 \\ 0 \\ 0 \end{Bmatrix} \quad (6)$$

For a nontrivial solution for the equations, the determinant of the coefficient matrix of the system of equations is set equal to zero, leading to the dispersion equation as

$$A_1\omega^6 + A_2\omega^4 + A_3\omega^2 + A_4 = 0 \quad (7)$$

where

$$A_1 = m_1m_2m_3$$

$$A_2 = -m_1(m_2+m_3)k_3 - m_3(m_2+m_1)k_2 - 2m_2m_3(1-\cos qL)k_1$$

$$A_3 = (m_1+m_2+m_3)k_2k_3 + 2(1-\cos qL)k_1[(m_2+m_3)k_3 + m_3k_2]$$

$$A_3 = -2(1-\cos qL)k_1k_2k_3$$

From the equation above, three branches of frequency ω can be obtained for a given dimensionless wave number qL. It is also evident that the dispersion curves of the two-resonator system are influenced by a number of parameters. It should be mentioned that although the above derivation is for the two-resonator acoustic metamaterial, similar analysis could be extended to the multiresonator acoustic metamaterial without any difficulty.

2.2 Band Gap Behavior. In this subsection, wave band gaps produced by the two-resonator mass-in-mass system are investigated for different mass and spring constant values. The band gap of the one-resonator mass-in-mass system studied by Huang et al. [24] is also included for comparison. Attention is focused on the roles played by the additional spring and mass parameters k_3 and m_3.

2.2.1 Effect of k_3 on Band Gap. Figures 2(*a*)–2(*d*) show the nondimensionalized dispersion curves of the two-resonator mass-in-mass system with $m_2/m_1=9$, $m_3/m_2=0.2$, and $k_2/k_1=2.0$. In the figures, $\omega_0=\sqrt{k_2/m_2}$ is the local resonance frequency of the one-resonator system. The lowest branch in the figures is called the acoustic wave mode, in which all the masses move in phase; the next higher branch is the optic wave mode, in which the masses m_2 and m_3 in the unit cell move out of phase. The dash lines represent the results from the two-resonator system and the solid lines are the results for the one-resonator system. Note that in Figs. 2(*a*)–2(*d*), only spring constant k_3 is varied with $k_3/k_2=0.01$, $k_3/k_2=0.1$, $k_3/k_2=2.0$, and $k_3/k_2=5.0$, respectively. The dispersion curves for the one-resonator mass-in-mass system with $m_2/m_1=9$ and $k_2/k_1=2.0$ are also shown in the figure.

From Figs. 2(*a*)–2(*d*), we note that the band gap behavior of the lattice system can be tailored. The first band gap created by the one-resonator system is in the range of $\omega=0.8\omega_0\sim3.2\omega_0$, and the second band gap is $\omega>5.2\omega_0$. By introducing the third mass-spring system (m_3 and k_3), an additional new band gap is created. For example, for $k_3/k_2=0.01$ shown in Fig. 2(*a*), a new band gap is created in the acoustic wave mode range $(0-0.8\omega_0)$ of the one-resonator mass-in-mass system. The range of the new band gap frequencies can be raised by increasing the spring constant k_3 without altering the original two band gaps. If the value of k_3 is increased to $k_3/k_2=0.1$, the new band gap is then created in the first original band gap $(0.8\omega_0-3.2\omega_0)$, as shown in Fig. 2(*b*). Figure 2(*c*) shows that the new band gap is created in the optic wave mode range $(3.4\omega_0-5.2\omega_0)$ when the spring constant k_3 increases to $k_3/k_2=0.1$. Figure 2(*d*) shows that the new band gap is created in the second band gap $(>5.2\omega_0)$. In this case, both the original (one-resonator) acoustic and optic wave modes are not influenced. It is noted that the third passing wave range is very narrow. Based on those results, it can be concluded that the relatively low ratio value of k_3/k_2 will mainly tailor and create new low frequency band gaps, and the relatively high ratio value will generate new high frequency band gaps.

2.2.2 Effect of m_3 on Band Gap. In addition to the spring constant k_3, mass m_3 may affect the band gap structure of the system. Figures 3(*a*) and 3(*b*) show the nondimensionalized dispersion curves of the two-resonator mass-in-mass system with $m_2/m_1=9$, $k_3/k_2=0.2$, and $k_2/k_1=2.0$. In the figures, only the value of mass m_3 is varied, i.e., $m_3/m_2=1.0$ and $m_3/m_2=5.0$.

By comparing the results in Figs. 3(*a*) and 3(*b*), it can be seen

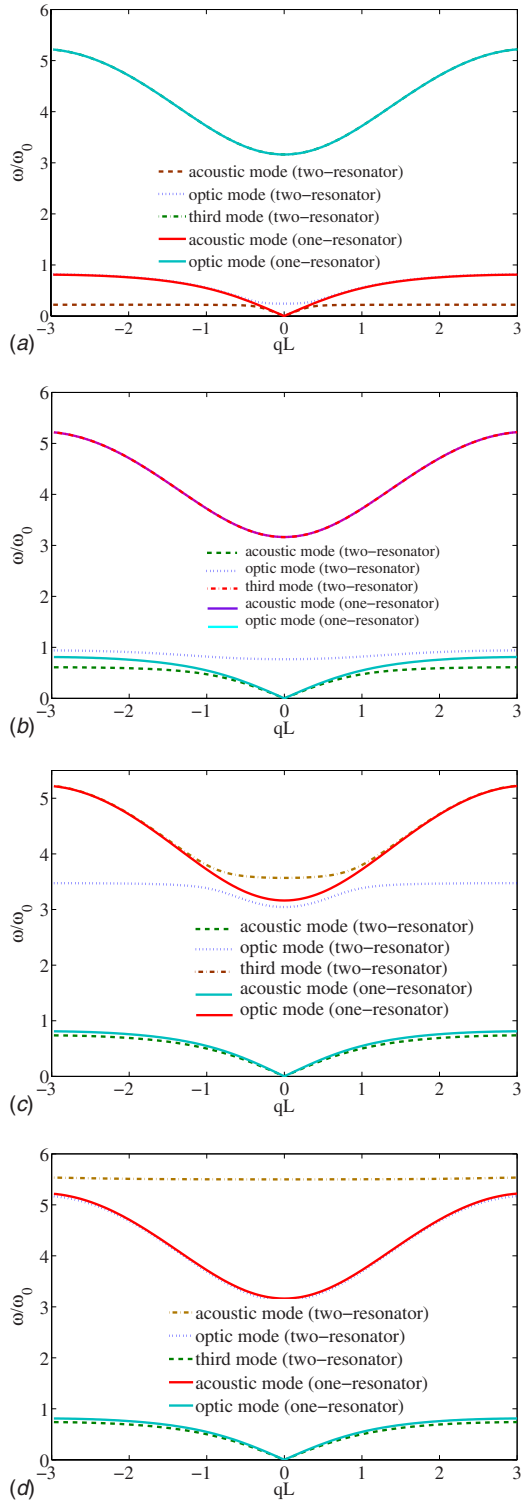

Fig. 2 Nondimensionalized dispersion curves for the one (solid line) and two-resonator (dash line) mass-in-mass systems with (*a*) $k_3/k_2=0.01$, (*b*) $k_3/k_2=0.1$, (*c*) $k_3/k_2=2.0$, and (*d*) $k_3/k_2=5.0$

that the additional mass m_3 can change the range of the new band gap. Figure 3(*a*) shows that the range of the band gap in the case $m_3/m_2=1.0$ is $0.24\omega_0$, lying between $0.38\omega_0$ and $0.62\omega_0$. For the case $m_3/m_2=5.0$, the range of the band gap is changed to around $0.32\omega_0$, see Fig. 3(*b*). Numerical results also show that the starting point of the lowest wave band gap is close to the local resonance frequency of mass 3, $\omega_3=\sqrt{k_3/m_3}$.

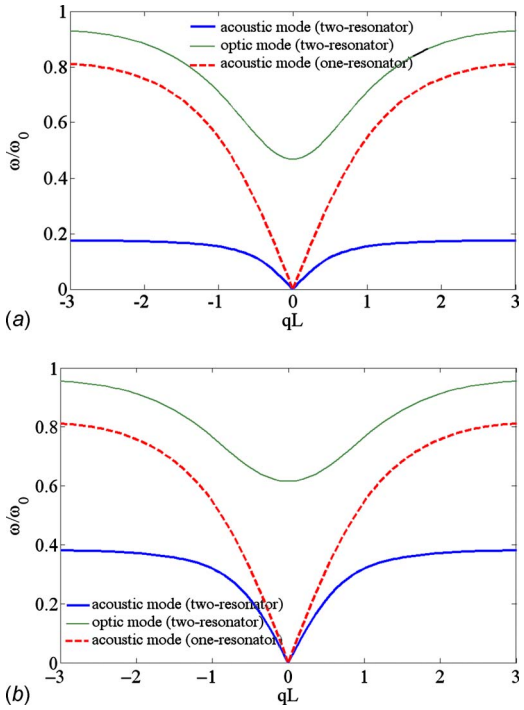

Fig. 3 Nondimensionalized dispersion curves for mass-in-mass systems (*a*) $m_3/m_2=1.0$ and (*b*) $m_3/m_2=5.0$

3 Negative Effective Mass

If the mass-in-mass unit is to be represented by a single mass, then the effective mass must be defined in order that the representative mass would produce the same displacement of m_1. In other words, the identity of the internal masses m_2 and m_3 would be ignored and its effect would be absorbed by the introduction of an effective mass m_{eff}. In this section, the two-resonator mass-in-mass lattice is represented by a classical monatomic lattice system. Consider an effective monatomic lattice system in which the unit cell is represented by a single effective masses m_{eff} connected by springs with spring constant k_1. The equation of motion for the effective mass at lattice point j is

$$m_{\text{eff}}\ddot{u}^{(j)} + k_1(2u^{(j)} - u^{(j+1)} - u^{(j-1)}) = 0 \tag{8}$$

The dispersion equation for harmonic waves can be readily obtained as

$$\omega^2 = \frac{2k_1(1-\cos(qL))}{m_{\text{eff}}} \tag{9}$$

If the effective monatomic lattice system is equivalent to the original mass-in-mass lattice system, then the dispersion curves of the two systems must be made identical. In that case, the effective mass m_{eff} can be determined by substituting Eq. (9) in the dispersion equation (Eq. (7)) of the original three body mass-in-mass system. Since both k_1 and ω^2 are positive in Eq. (9), a negative effective mass density is possible only when $1-\cos(qL)$ turns negative, i.e., the dimensionless wave number qL is complex. Mathematically, this is equivalent to the phononic band gap where no real-valued wave number solution exists for the dispersion equation. Hence, we should expect no harmonic wave propagation if the effective mass density is negative. In other words, a negative effective mass in the equivalent mass-spring lattice system yields significant spatial attenuation of the wave amplitude.

For material constants $m_2/m_1=9$, $m_3/m_2=0.2$, and $k_2/k_1=2.0$, the dimensionless effective mass $m_{\text{eff}}/m_{\text{st}}$ is plotted in Figs. 4(*a*) and 4(*b*) as a function of ω/ω_0 for the cases of $k_3/k_2=0.1$ and $k_3/k_2=2.0$, respectively. The dimensionless effective mass for the

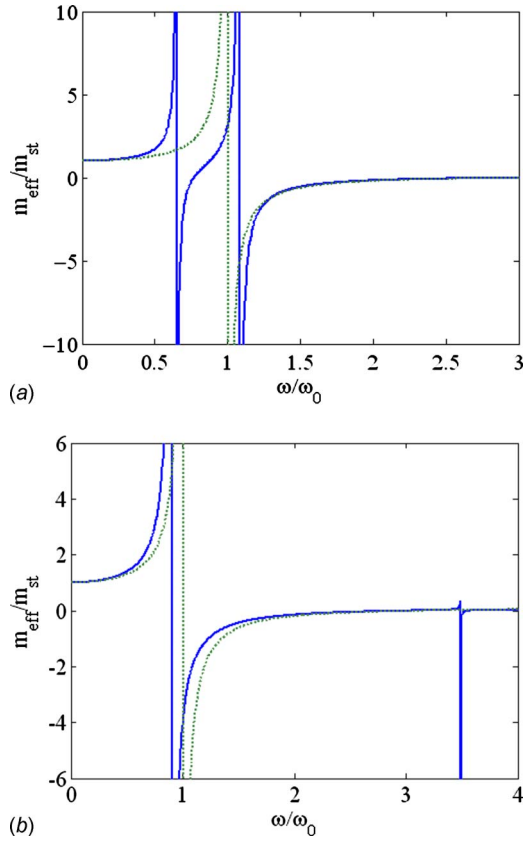

Fig. 4 Dimensionless effective mass m_{eff}/m_{st} as a function of ω/ω_0 (one-resonator: dotted line; two-resonator: solid line): (*a*) $k_3/k_2=0.1$ and (*b*) $k_3/k_2=2.0$

one-resonator mass-in-mass system is also included for comparison. In the figures, $m_{st}=m_1+m_2+m_3$ is defined for the two-resonator mass-in-mass system and $m_{st}=m_1+m_2$ for the one-resonator system. For the two-resonator system, the effective mass becomes negative in two frequency ranges, in which two band gaps exist. Numerical results also show that negative effective mass occurs near the local resonance frequencies for both one-resonator and two-resonator mass-in-mass systems. However, the starting frequency of the first band gap of the one-resonator system is always at $\omega/\omega_0=1.0$, while the starting frequency for the first band gap of the two-resonator system is $\omega/\omega_0=0.8$. In other words, the negative effective mass should be in the range of the band gap. However, in the band gap range, some positive effective mass can exist. Besides, at the long wavelength limit ($\omega\to 0$), the effective mass m_{eff} approaches m_{st} as expected.

4 Microstructure Continuum Representation of the Mass-in-Mass System

The mass-in-mass and the equivalent monatomic lattice models considered in Sec. 3 are discrete systems. The classical continuum theory with one degree of freedom and constant material properties cannot directly represent the original mass-in-mass system because the additional degrees of freedom of the internal masses m_2 and m_3 are not considered. Therefore, the classical continuum theory is not adequate for describing the deformation of materials with microstructures, if local deformation/motion in the microstructure is desired. Microstructure continuum theories, which employ additional kinematic variables are more suitable to represent the mass-in-mass system. In this study, we introduce a microstructure continuum model in the form of displacement and microdeformation variables.

4.1 Microstructure Continuum Model. Consider the unit cell in the three body mass-in-mass lattice, as shown in Fig. 1. In a general motion, the deformation and kinetic energies in the unit cell, respectively, are

$$W^{(j)}=\frac{1}{2}[k_1(u_1^{(j+1)}-u_1^{(j)})^2+k_2(u_2^{(j)}-u_1^{(j)})^2+k_3(u_3^{(j)}-u_2^{(j)})^2] \tag{10}$$

and

$$T^{(j)}=\frac{1}{2}[m_1(\dot{u}_1^{(j)})^2+m_2(\dot{u}_2^{(j)})^2+m_3(\dot{u}_3^{(j)})^2] \tag{11}$$

To derive a continuum model that can represent the three body lattice system, we now introduce the global displacement $U(x)\equiv u_1(x)$, microdeformation variables $\Phi_{12}(x)\equiv(u_2-u_1)/L$, and $\Phi_{13}(x)\equiv(u_3-u_1)/L$, which give the displacements of all m_1, m_2, and m_3 mass points, respectively. The global displacement $U(x)$ is the displacement at the center of the representative volume element (RVE) (the average displacement), while $\Phi_{12}(x)$ and $\Phi_{13}(x)$ characterize the relative micromotions of mass m_2 and m_3.

Using a two-term Taylor series expansion for the global displacement, we have

$$u_1^{(j+1)}=U(x+L)=U(x)+\frac{\partial U}{\partial x}L \tag{12}$$

Assume that the one-dimensional equivalent continuum has a unit cross-sectional area and defines global normal strain $E=\partial U/\partial x$, then the deformation energy density W can be expressed solely in terms of the three field variables E, $\Phi_{12}(x)$, and $\Phi_{13}(x)$ as

$$W=\frac{1}{2L}[k_1(LE)^2+k_2(L\Phi_{12})^2+k_3L^2(\Phi_{13}-\Phi_{12})^2] \tag{13}$$

$$T=\frac{1}{2L}[m_1(\dot{U})^2+m_2(\dot{U}+L\dot{\Phi}_{12})^2+m_3(\dot{U}+L\dot{\Phi}_{13})^2] \tag{14}$$

Subsequently, the Cauchy stress and relative stresses are introduced by

$$\sigma=\frac{\partial W}{\partial E}=k_1LE \tag{15}$$

and

$$\sigma_{12}^R=\frac{\partial W}{\partial \Phi_{12}}=(k_2+k_3)L\Phi_{12}-k_3L\Phi_{13} \tag{16}$$

$$\sigma_{13}^R=\frac{\partial W}{\partial \Phi_{13}}=k_3L\Phi_{13}-k_3L\Phi_{12} \tag{17}$$

respectively. Equations (15)–(17) are the constitutive equations of the microstructure continuum model.

The final step to complete the continuum model is to derive the equations of motion using the Hamilton's principle, that is

$$\delta\int_{t_0}^{t_1}\int_V (T-W)dVdt=0 \tag{18}$$

We obtain

$$\rho\ddot{U}+m_2\ddot{\Phi}_{12}+m_3\ddot{\Phi}_{13}-k_1L\frac{\partial^2 U}{\partial x^2}=0 \tag{19}$$

$$m_2L\ddot{\Phi}_{12}+m_2\ddot{U}+(k_2+k_3)L\Phi_{12}-k_3L\Phi_{13}=0 \tag{20}$$

$$m_3L\ddot{\Phi}_{13}+m_3\ddot{U}+k_3L\Phi_{13}-k_3L\Phi_{12}=0 \tag{21}$$

where

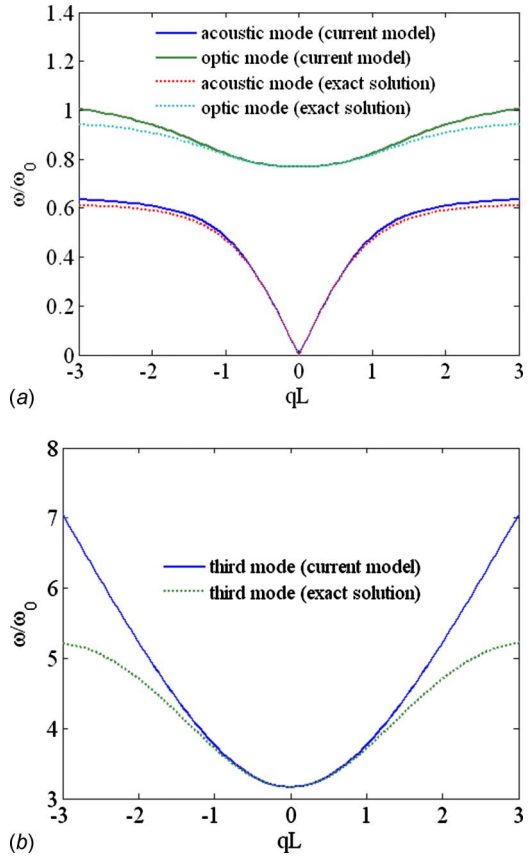

Fig. 5 Dispersion curves obtained from the microstructure continuum model compared with that from the two-resonator mass-in-mass lattice model: (*a*) acoustic mode and optic mode, and (*b*) third mode

$$\rho = \frac{m_1 + m_2 + m_3}{L}$$

4.2 Evaluation of the Microstructure Continuum Model. To evaluate the accuracy of the representation of the mass-in-mass system by the microstructure continuum model, we consider harmonic wave propagation of the form

$$U = A_1 e^{i(qx-\omega t)} \tag{22}$$

$$\Phi_{12} = A_2 e^{i(qx-\omega t)} \tag{23}$$

$$\Phi_{13} = A_3 e^{i(qx-\omega t)} \tag{24}$$

where A_α ($\alpha=1,2,3$) is the complex wave amplitude to be determined. Substituting the expressions above in the equations of motion (18)–(21), we obtain the dispersion equation as

$$\begin{bmatrix} k_1 L q^2 - \rho\omega^2 & -m_2\omega^2 & -m_3\omega^2 \\ -m_2\omega^2 & (k_2+k_3) - m_2 L\omega^2 & -k_3 L \\ -m_3\omega^2 & -k_3 L & k_3 L - m_3 L\omega^2 \end{bmatrix} \begin{Bmatrix} A_1 \\ A_2 \\ A_3 \end{Bmatrix} = \begin{Bmatrix} 0 \\ 0 \\ 0 \end{Bmatrix} \tag{25}$$

Dispersion curves obtained with the microstructure continuum model and with the original two-resonator lattice model are shown Fig. 5. The material properties used in Fig. 5 are: $m_2/m_1=9$, $m_3/m_2=0.2$, $k_2/k_1=2.0$, and $k_3/k_2=0.1$. It is evident that the microstructure continuum model describes the dispersion behavior of the mass-in-mass system very well, especially for the acoustic mode. As for the optic mode and the third mode, the accuracy is fairly accurate up to $qL=1$. This means that the continuum model is accurate for wavelengths greater than six times the lattice spacing (L) for the optic mode and the third mode. It is of interest to note that there is no negative effective mass used in the microstructure model.

5 Summary

Using a two-resonator mass-in-mass lattice system, we have shown that it is possible to create acoustic band gaps to forbid wave propagation in several ranges of frequency. It was found that the major band gap is determined mainly by the outer mass of the mass-in-mass lattice system, and the minor band gap can be achieved by the change in the microstructure parameters such as inner mass-spring constants. If the multiple mass lattice system is treated as an effective single mass lattice system, then the effective mass would become negative in the band gap frequencies. Finally, a microstructure continuum model was proposed to represent the two-resonator lattice system. This microstructure continuum model was found capable of producing accurate dispersion curves, and also capture the band gap structure of the original two-resonator lattice system.

References

[1] Veselago, V. G., 1968, "The Electrodynamics of Substances With Simultaneously Negative Values of ε and μ ," Sov. Phys. Usp., **10**, pp. 509–514.
[2] Smith, D. R., Pendry, J. B., and Wiltshire, M. C. K., 2004, "Metamaterials and Negative Refractive Index," Science, **305**, pp. 788–792.
[3] Pendry, J. B., Holden, A. J., Robbins, D. J., and Stewart, W. J., 1999, "Magnetism From Conductors and Enhanced Nonlinear Phenomena," IEEE Trans. Microwave Theory Tech., **47**, pp. 2075–2084.
[4] Cummer, S. A., and Schurig, D., 2007, "One Path to Acoustic Cloaking," New J. Phys., **9**, pp. 45–52.
[5] Vukusic, P., and Sambles, J. R., 2003, "Photonic Structures in Biology," Nature (London), **424**, pp. 852–855.
[6] Linden, S., Enkrich, C., Wegener, M., Zhou, J., Koschny, T., and Soukoulis, C. M., 2004, "Magnetic Response of Metamaterials at 100 Terahertz," Science, **306**, pp. 1351–1353.
[7] Smirnova, E. I., Mastovsky, I., Shapiro, M. A., Temkin, R. J., Earley, L. M., and Edwards, R. L., 2005, "Fabrication and Cold Test of Photonic Band Gap Resonators and Accelerator Structures," Phys. Rev. ST Accel. Beams, **8**, p. 091302.
[8] Liu, Z., Chan, C. T., and Sheng, P., 2005, "Analytic Model of Phononic Crystals With Local Resonances," Phys. Rev. B, **71**, p. 014103.
[9] Mei, J., Liu, Z., Wen, W., and Sheng, P., 2006, "Effective Mass Density of Fluid-Solid Composites," Phys. Rev. Lett., **96**, p. 024301.
[10] Wu, Y., Lai, Y., and Zhang, Z., 2007, "Effective Medium Theory for Elastic Metamaterials in Two Dimensions," Phys. Rev. B, **76**, p. 205313.
[11] Sigalas, M. M., and Economou, E. N., 1992, "Elastic and Acoustic Wave Band Structure," J. Sound Vib., **158**, pp. 377–382.
[12] Poulton, C. G., Movchan, A. B., McPhedran, R. C., Nicorovici, N. A., and Antipov, Y. A., 2000, "Eigenvalue Problems for Doubly Periodic Elastic Structures and Phononic Band Gaps," Proc. R. Soc. London, Ser. A, **456**, pp. 2543–2559.
[13] Kushwaha, M. S., Halevi, P., Dobrzynski, L., and Djafari-Rouhani, B., 1993, "Acoustic Band Structure of Periodic Elastic Composites," Phys. Rev. Lett., **71**, pp. 2022–2025.
[14] Martinsson, P. G., and Movchan, A. B., 2003, "Vibration of Lattice Structures and Phononic Band Gaps," Q. J. Mech. Appl. Math., **56**, pp. 45–64.
[15] Sigalas, M. M., 1998, "Defect States of Acoustic Waves in a Two-Dimensional Lattice of Solid Cylinders," J. Appl. Phys., **84**, pp. 3026–3030.
[16] Yang, S. X., Page, J. H., Liu, Z. Y., Cowan, M. L., Chan, C. T., and Sheng, P., 2004, "Focusing of Sound in a 3D Phononic Crystal," Phys. Rev. Lett., **93**, p. 024301.
[17] Hu, X. H., Chan, C. T., and Zi, J., 2005, "Two-Dimensional Sonic Crystals With Helmholtz Resonators," Phys. Rev. E, **71**, p. 055601.
[18] Fang, N., Xi, D. J., Xu, J. Y., Ambati, M., Srituravanich, W., Sun, C., and Zhang, X., 2006, "Ultrasonic Metamaterials With Negative Modulus," Nature Mater., **5**, pp. 452–456.
[19] Zhang, X., and Liu, Z., 2004, "Negative Refraction of Acoustic Waves in Two-Dimensional Phononic Crystals," Appl. Phys. Lett., **85**, pp. 341–343.
[20] Liu, Z., Zhang, X., Mao, Y., Zhu, Y. Y., Yang, Z., Chan, C. T., and Sheng, P., 2000, "Locally Resonant Sonic Materials," Science, **289**, pp. 1734–1736.
[21] Li, J., and Chan, C. T., 2004, "Double-Negative Acoustic Metamaterial," Phys. Rev. E, **70**, p. 055602.
[22] Milton, G. W., and Willis, J. R., 2007, "On Modifications of Newton's Second Law and Linear Continuum Elastodynamics," Proc. R. Soc. London, Ser. A, **463**, pp. 855–880.
[23] Yao, S. S., Zhou, X. M., and Hu, G. K., 2008, "Experimental Study on Negative Effective Mass in a 1D Mass-Spring System," New J. Phys., **10**, p. 043020.
[24] Huang, H. H., Sun, C. T., and Huang, G. L., 2009, "On the Negative Effective

Mass Density in Acoustic Metamaterials," Int. J. Eng. Sci., **47**, pp. 610–617.
[25] Vincent, J. H., 1898, "On the Construction of a Mechanical Model to Illustrate Helmholtz's Theory of Dispersion," Philos. Mag., **46**, pp. 557–563.
[26] Lazarov, B. S., and Jensen, J. S., 2007, "Low-Frequency Band Gaps in Chains With Attached Non-Linear Oscillators," Int. J. Non-Linear Mech., **42**, pp. 1186–1193.
[27] Sun, C. T., and Huang, G. L., 2007, "Modeling Heterogeneous Media With Microstructures of Different Scales," ASME J. Appl. Mech., **74**, pp. 203–209.
[28] Huang, G. L., and Sun, C. T., 2007, "Continuum Modeling of Solids With Micro/Nanostructures," Philos. Mag., **87**, pp. 3689–3707.